

This is the accepted manuscript made available via CHORUS. The article has been published as:

## Determination of the deuterium-tritium branching ratio based on inertial confinement fusion implosions

Y. Kim *et al.*

Phys. Rev. C **85**, 061601 — Published 25 June 2012

DOI: [10.1103/PhysRevC.85.061601](https://doi.org/10.1103/PhysRevC.85.061601)

# Determination of the D-T Branching Ratio based on Inertial Confinement Fusion Implosions

Y. Kim, J. M. Mack, H. W. Herrmann, C. S. Young, G. M. Hale, S. Caldwell, N. M. Hoffman, S. C. Evans, T. J. Sedillo, A. McEvoy, J. Langenbrunner, H. H. Hsu, M. A. Huff, and S. Batha  
*Los Alamos National Laboratory, Los Alamos, New Mexico 87545, USA*

C. J. Horsfield, M. S. Rubery, and W. J. Garbett  
*Atomic Weapons Establishment, Aldermaston, Reading, Berkshire, RG7 4PR, U.K.*

W. Stoeffl, E. Grafil, L. Bernstein, J. A. Church, and D. B. Sayre  
*Lawrence Livermore National Laboratory, Livermore, California 94550, USA*

M. J. Rosenberg, C. Waugh, H. G. Rinderknecht, M. Gatu Johnson, A. B. Zylstra, J. A. Frenje, D. T. Casey, and R. D. Petrasso  
*Plasma Science and Fusion Center, Massachusetts Institute of Technology, Cambridge, Massachusetts 02139, USA*

E. Kirk Miller  
*National Security Technologies, LLC, Special Technologies Laboratory, Santa Barbara, California 93111, USA*

V. Yu Glebov, C. Stoeckl, and T. C. Sangster  
*Laboratory for Laser Energetics, University of Rochester, Rochester, New York 14623, USA*

The D-T gamma-to-neutron branching ratio ( ${}^3\text{H}(\text{d},\gamma){}^5\text{He}/{}^3\text{H}(\text{d},\text{n}){}^4\text{He}$ ) has been determined at inertial confinement fusion (ICF) conditions, where the center-of-mass energy of 14 - 24 keV is lower than in previous accelerator-based experiments. A D-T branching ratio value of  $(4.2 \pm 2.0) \times 10^{-5}$  was determined by averaging the results of two methods: 1) a direct measurement of ICF D-T  $\gamma$ -ray and neutron emissions using absolutely-calibrated detectors, and 2) a separate cross-calibration against the D- ${}^3\text{He}$  gamma-to-proton branching ratio ( ${}^3\text{He}(\text{d},\gamma){}^5\text{Li}/{}^3\text{He}(\text{d},\text{p}){}^4\text{He}$ ). Neutron-induced backgrounds are significantly reduced as compared to traditional beam-target accelerator-based experiments due to the short pulse nature of ICF implosions and the use of gas Cherenkov  $\gamma$ -ray detectors with fast temporal responses and inherent energy thresholds. These measurements of the D-T branching ratio in an ICF environment test several theoretical assumptions about the nature of  $A = 5$  systems, including the dominance of the  $3/2^+$  resonance at low energies, the presence of the broad first excited state of  ${}^5\text{He}$  in the spectra, and the charge-symmetric nature of the capture processes in the mirror systems  ${}^5\text{He}$  and  ${}^5\text{Li}$ .

At the National Ignition Facility (NIF), high energy lasers (up to 1.8 MJ) are used to implode capsules of cryogenically-layered deuterium (D) and tritium (T) fuel enclosed in high-Z hohlraums. The ultimate goal is to achieve self-sustaining fusion burn, requiring extreme fuel core conditions (e.g., fuel areal density  $> 1 \text{ g/cm}^2$ ) that have been unattainable in past laboratory inertial confinement fusion (ICF) experiments [1]. One key to achieving ignition is an accurate understanding of the fusion reaction history as it relates to capsule performance [2]. The D-T fusion reaction emits two strong candidates for diagnosing thermonuclear burn: 14.1 MeV neutrons and high-energy (10 - 17 MeV)  $\gamma$ -rays. Fusion  $\gamma$ -ray diagnostics have potential advantages over neutron measurements because  $\gamma$ -rays emerge from the implosion relatively unperturbed and do not Doppler broaden in transit to a detector. To obtain absolute fusion reaction history out of  $\gamma$ -ray measurements, either a cross-calibration against highly accurate neutron yield measurement is required or precise D-T gamma-to-neutron branching ratio information at ICF conditions is needed.

The D-T branching ratio is also of fundamental interest from a nuclear physics perspective. The fusion of D and T

produces an excited  ${}^5\text{He}$  nucleus, which de-excites via at least three branches [3]:

$$D + T \rightarrow {}^5\text{He}^* \rightarrow {}^4\text{He}(3.5 \text{ MeV}) + n(14.1 \text{ MeV}) \quad (1)$$

$$D + T \rightarrow {}^5\text{He}^* \rightarrow {}^5\text{He} + \gamma_0(16.75 \text{ MeV}) \quad (2)$$

$$D + T \rightarrow {}^5\text{He}^* \rightarrow {}^5\text{He}^* + \gamma_1(\sim 13.5 \text{ MeV}) \quad (3)$$

The most common mode results in the emission of a 3.5 MeV alpha particle and a 14.1 MeV neutron [Eq. (1)]. Less frequent modes involve the excited  ${}^5\text{He}$  nucleus relaxing to the ground state via the emission of a 16.75 MeV  $\gamma$ -ray,  $\gamma_0$  [Eq. (2)] or to the  $1^{\text{st}}$  excited state via emission of a broad  $\gamma$ -ray line at approximately 13.5 MeV,  $\gamma_1$  [Eq. (3)] [4]. While  $\gamma_0$  has been measured directly in beam-target experiments,  $\gamma_1$  has been more elusive due in part to the 14.1 MeV neutron-induced  $\gamma$ -ray background present in such experiments [5 - 7].

While the D-T gamma-to-neutron branching ratio has been measured via accelerator-based beam-target experiments for at least 50 years, the published values for the yield ratio of the  $\gamma$ -ray branches [Eqs. (2) and (3)] to the neutron branch [Eq. (1)] range from  $1 \times 10^{-5}$  to  $3 \times 10^{-4}$  [5-12]. The disparity in these data can likely be explained by 1) an undetermined D-T fusion  $\gamma$ -ray energy spectrum, and 2) an intractable 14.1

MeV neutron-induced  $\gamma$ -ray background, produced by solid targets in beam-target experiments. In contrast, ICF provides a pulsed D-T fusion  $\gamma$ -ray source with interferences that are either negligible or that can be excluded from the signal.

In this paper, we determine the D-T branching ratio by two methods at ICF conditions. The first method is based on absolute calibration of  $\gamma$ -ray and neutron measurements in ICF D-T experiments. To lessen the possibility of unknown systematic uncertainties in absolute  $\gamma$ -ray detection, the second method relies on cross calibration to the better known D- $^3\text{He}$  gamma-to-proton branching ratio. Based on a weighted average of the two methods, the D-T branching ratio is determined to be  $(4.2 \pm 2.0) \times 10^{-5}$ , where both  $\gamma_0$  and  $\gamma_1$  are included.

ICF implosions were measured at the University of Rochester OMEGA Laser Facility. To achieve the implosions, 60 laser beams (351 nm), with a total energy of 23 – 28 kJ, were focused on the target at chamber center (TCC) for a duration of 1 ns. For the D-T experiments, the target was a CH plastic shell of thickness 15 – 30  $\mu\text{m}$  and an outer diameter of approximately 1 mm, filled with 15 atm of gaseous D-T fuel in a ratio of D/T  $\sim$  65/35. Because the fuel is gaseous and the capsule wall is thin, implosion areal density remains low and neutron-induced  $\gamma$ -ray backgrounds from the target itself are greatly reduced. Known high-energy background  $\gamma$ -rays include those emitted from the inelastic scattering in the shell ( $^{12}\text{C}(n,n'\gamma)$  at 4.44 MeV [13]) and from radiative capture in the fuel (D(n, $\gamma$ ) at 15.58 MeV [14]). The intensity of the D(n,  $\gamma$ )  $\gamma$ -ray signal depends on fuel  $\rho R$  (the radial integral of the fuel mass density, whose value from simulation is in the range of 6 – 8  $\text{mg}/\text{cm}^2$ ), and is estimated to contribute  $< 0.1\%$  for these non-cryogenic gas-filled capsules at OMEGA [15]. Existing neutron-induced  $\gamma$ -ray data for  $^{12}\text{C}$  indicates that the  $^{12}\text{C}(n, n'\gamma)$  reaction has approximately 4 orders of magnitude greater intensity than other  $\gamma$ -ray producing channels in  $^{12}\text{C}$  [16]. Given these data, and the limited areal density of  $^{12}\text{C}$  in the compressed plastic capsules (approximately 40  $\text{mg}/\text{cm}^2$  at OMEGA), only the 4.44 MeV  $\gamma$ -ray is significant. This background, though significant, can be discriminated by using energy thresholds inherent to Cherenkov  $\gamma$ -ray detectors.

The Gas Cherenkov Detector (GCD) [17-19] and Gamma Reaction History (GRH) [20, 21] diagnostics were designed for this purpose. GCD converts  $\gamma$ -rays to Compton electrons as they interact with a 1.5-cm-thick, 7-cm-diameter beryllium disk. Pressurized  $\text{CO}_2$  (variable up to 100 psia) acts as the dielectric medium, producing optical Cherenkov light, which is then relayed via Cassegranian optics to a Photek ultra-fast, microchannel-plate photo-multiplier tube (PMT). GRH operates in a similar manner as GCD, but with a 1.0-cm-thick, 12.7-cm-diameter aluminium converter, and  $\text{SF}_6$  (up to 200 psia) as the dielectric medium. To isolate D-T fusion  $\gamma$ -rays from the 4.44 MeV background, the  $\text{CO}_2$  gas pressure in GCD was fixed at 100 psia corresponding to a Cherenkov production energy

threshold of 6.3 MeV, while in GRH, the  $\text{SF}_6$  gas pressure was set to 87 psia, corresponding to an energy threshold of 5 MeV. Other undesirable neutron-induced backgrounds were eliminated through high-bandwidth electronics, which allowed D-T fusion  $\gamma$ -rays to be detected before 14.1 MeV neutrons had a chance to interact with masses surrounding the target, including the detectors themselves.

Figure 1 shows the time-integrated GCD and GRH  $\gamma$ -ray signals normalized by PMT gain and PMT quantum efficiency, as a function of absolute neutron yield. The data were obtained from a total of 22 OMEGA implosions taken between 2008 and 2011. The absolute D-T neutron yield was measured by using the neutron time-of-flight (nTOF-12m) OMEGA facility diagnostic [22] to an uncertainty of less than 5 %, and  $\gamma$ -rays were measured with GCD installed on an OMEGA Ten Inch Manipulator (TIM) set at a detector front-to-TCC distance of 20 cm, and GRH on the chamber wall with a TCC to detector distance of 187 cm. The time-integrated signal  $S_\gamma^{DT}(E_{thr})$  in units of volt-seconds ( $V \cdot s$ ) results from the detector response  $R(E; E_{thr})$  to the D-T fusion  $\gamma$ -ray yield  $Y_\gamma^{DT}$  and an assumed D-T fusion  $\gamma$ -ray spectrum  $I_\gamma^{DT}(E)$  (normalized to one) at a given energy threshold  $E_{thr}$ . It can be written:

$$\begin{aligned} S_\gamma^{DT}(E_{thr}) &= Y_\gamma^{DT} \int_{E_{thr}}^{\infty} I_\gamma^{DT}(E) R(E; E_{thr}) dE \\ &= Y_n^{DT} B_{\gamma/n}^{DT} (\Delta\Omega / 4\pi) Q G e r \int_{E_{thr}}^{\infty} I_\gamma^{DT}(E) R(E; E_{thr}) dE, \end{aligned} \quad (4)$$

where  $Y_n^{DT}$  is the measured neutron yield,  $B_{\gamma/n}^{DT} = Y_\gamma^{DT} / Y_n^{DT}$  is the D-T branching ratio,  $\Delta\Omega / 4\pi$  is the solid angle fraction of the converter plate (GCD's  $\Delta\Omega / 4\pi = 1.1 \times 10^{-2}$  and GRH's  $\Delta\Omega / 4\pi = 2.9 \times 10^{-4}$ ),  $Q$  is the PMT quantum efficiency to the UV/visible Cherenkov emission spectrum which reaches the PMT photocathode (typically  $\sim 15\%$ ),  $G$  is the PMT gain (typically  $10^4 - 10^6$ ),  $e = 1.602 \times 10^{-19}$  C is the charge of an electron, and  $r = 50$  ohm is the circuit resistance.  $R(E; E_{thr})$  is the response of the Cherenkov gas cell to  $\gamma$ -rays of energy  $E$ , in units of productive Cherenkov photons/incident  $\gamma$ -ray. Thus, the normalized  $\gamma$ -ray signal,  $S_\gamma^{iDT}(E_{thr}) = S_\gamma^{DT}(E_{thr}) / (Q G e r \Delta\Omega / 4\pi)$ , is proportional to  $Y_n^{DT}$ .

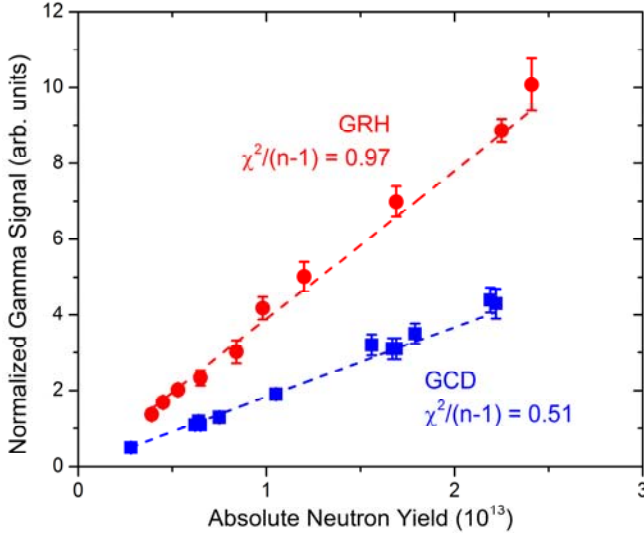


Figure 1: (Color online) Time-integrated and normalized GRH (top) and GCD (bottom)  $\gamma$ -ray signals ( $S_{\gamma}^{DT}(E_{thr})$ ) as a function of absolute neutron yield, obtained from 22 OMEGA implosions.  $S_{\gamma}^{DT}(E_{thr})$  increases linearly with neutron yield, indicating constant gamma-to-neutron branching ratio. From Eq. (5), the branching ratio can be determined by calibrating detector response.

In Figure 1, it can be seen that normalized  $\gamma$ -ray signals from GCD and GRH increase linearly with neutron yield, indicating a constant gamma-to-neutron branching ratio. Inverting Eq. (4),  $B_{\gamma/n}^{DT}$  can be inferred from the expression:

$$B_{\gamma/n}^{DT} = \frac{S_{\gamma}^{DT}(E_{thr}) / Y_n^{DT}}{\int_{E_{thr}}^{\infty} I_{\gamma}^{DT}(E) R'(E; E_{thr}) dE}. \quad (5)$$

The spectral shapes of the  $\gamma_1$  and  $\gamma_0$  lines have been determined theoretically using an R-matrix analysis [4, 23]. Figure 1 in Ref. 4 indicates that the D-T  $\gamma$ -ray spectrum consists of more than just a single line at 16.75 MeV corresponding to de-excitation of the  $^5\text{He}^*$  nucleus to the ground state. D-T fusion  $\gamma$ -rays resulting from the transition of  $^5\text{He}^*$  down to the first excited state also contribute to the spectrum. Recently, the ratio of these lines ( $\gamma_1/\gamma_0$ ) has been experimentally determined to be in the range of 2 - 3 based on Cherenkov energy-thresholding scans also conducted at OMEGA with GCD [24]. The experimental spectrum is used to determine  $I_{\gamma}^{DT}(E)$  and a detailed description will be given in a later publication.

An absolute determination of  $B_{\gamma/n}^{DT}$ , requires accurate GCD and GRH responses  $R'(E; E_{thr})$ . To obtain these values, two independent Monte Carlo computer codes, ACCEPT [4] and GEANT4 [25] were modified by adding time & wavelength dependent Cherenkov and optical transition radiation (OTR). Both simulation codes have been validated against measurements at the High-Intensity Gamma-Ray Source (HIγS), where GCD and GRH were placed in a collimated (1 cm diameter) mono-energetic  $\gamma$ -ray beam (at 4.4, 10.01, or 16.86 MeV), and the Cherenkov light from GCD and

GRH was measured with the same instrumentation fielded at OMEGA. The GCD and GRH code results (ACCEPT and GEANT4) are consistently higher than the HIγS data. A factor of approximately 0.7 allows the GCD and GRH models to match the measurement. Keeping a correction factor of 0.7, the simulations were then extended to the OMEGA configuration and used to compute the absolute detector response for each of the detectors. Figure 2 shows that D-T branching ratios obtained from GCD (square symbol) and from GRH (circle symbol) based on these responses are in agreement. An absolute D-T branching ratio of  $(4.3 \pm 1.8) \times 10^{-5}$  with 7.3 % random uncertainty and 33.9 % systematic uncertainty is inferred by a weighted average of the results from the two detectors.

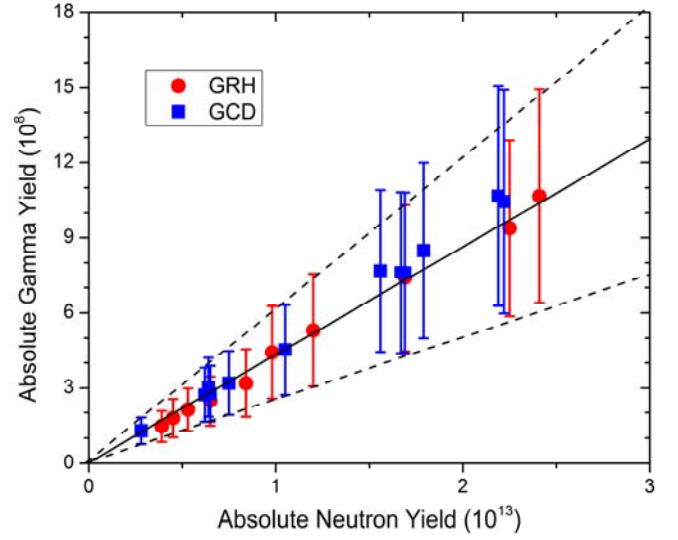


Figure 2: (Color online) Absolute  $\gamma$ -ray yields obtained from GCD (square symbol) and from GRH (circle symbol) are in agreement. After a weighted average, the slopes of the lines reveal a D-T branching ratio of  $(4.3 \pm 1.8) \times 10^{-5}$ . The solid line corresponds to a branching ratio of  $4.3 \times 10^{-5}$ . The lower and upper lines show the range of branching ratio,  $(2.5 - 6.1) \times 10^{-5}$ .

To obtain the D-T branching ratio from the second approach, the D- $^3\text{He}$  cross-calibration method used by Kosiara *et al.* [9] and Kammeraad *et al.* [7] was adopted. D- $^3\text{He}$  fusion is similar to D-T fusion (Eqs. 1 - 3) with the exception that  $^5\text{He}^*$  is replaced with its mirror nucleus,  $^5\text{Li}^*$ . The energy level structures of  $^5\text{He}^*$  and  $^5\text{Li}^*$  are very close to each other, and thus their  $\gamma$ -ray energy spectra are similar [7]. The D-T neutron emission is replaced by a 14.7 MeV proton in the D- $^3\text{He}$  reaction, further reducing problems associated with the 14.1 MeV neutron backgrounds found in beam-target D-T gamma-to-neutron branching ratio experiments. Assuming the  $\gamma$ -ray spectra are identical for  $^5\text{He}^*$  and  $^5\text{Li}^*$ , and without knowing the absolute detector response  $R'(E; E_{thr})$ , we can infer  $B_{\gamma/n}^{DT}$  as,

$$B_{\gamma/n}^{DT} = B_{\gamma/p}^{D^3\text{He}} \frac{S_{\gamma}^{DT}(E_{thr}) / Y_n^{DT}}{S_{\gamma}^{D^3\text{He}}(E_{thr}) / Y_p^{D^3\text{He}}}. \quad (6)$$

D- $^3\text{He}$  and D-T implosion experiments were performed on the same day at OMEGA, over two campaigns

(September, 2010 and May, 2011). The D-<sup>3</sup>He capsules were glass, and filled with 6 atm of D<sub>2</sub> and 12 atm of <sup>3</sup>He. Gamma-ray measurements were made on both types of implosions with the same GCD instrument. Neutron yield measurements were made for the D-T implosions as before, while proton yield measurements were made for the D-<sup>3</sup>He implosions. In contrast to the neutron yield measurements, proton yield diagnostics in ICF implosions need to account for anisotropic fluence effects associated with electromagnetic fields around the capsule, which deflect charged fusion products [26]. To ensure a properly angle-averaged proton yield, seven proton diagnostics were fielded at selected locations around the target chamber. Included were Charged Particles Spectrometers (CPS-1 and -2), Wedge Range Filter (WRF) proton spectrometers, range-filtered CR-39, and the Magnetic Recoil Spectrometer (MRS) [27]. Uncertainties in the global proton yield are kept to less than 10 % by averaging all of the proton data.

Figure 3 shows GCD reaction histories for D-<sup>3</sup>He (top) and D-T (bottom) implosions normalized for proton and neutron yields, respectively. Integrating the signals from D-<sup>3</sup>He and D-T implosions, we obtain  $\frac{S_{\gamma}^{DT}(E_{thr})/Y_n^{DT}}{S_{\gamma}^{D^3He}(E_{thr})/Y_p^{D^3He}} = \frac{B_{\gamma/n}^{DT}}{B_{\gamma/p}^{D^3He}} = (0.31 \pm 0.08)$ . Applying the published value of total  $(= \gamma_0 + \gamma_1) B_{\gamma/p}^{D^3He} = (12.5 \pm 4.2) \times 10^{-5}$  from Cecil *et al.* [28] to these data, results in a D-T branching ratio of  $B_{\gamma/n}^{DT} = (3.9 \pm 2.3) \times 10^{-5}$  for the cross-calibration approach, where random uncertainty is 25.4 % and systematic uncertainty is 33.6 %.

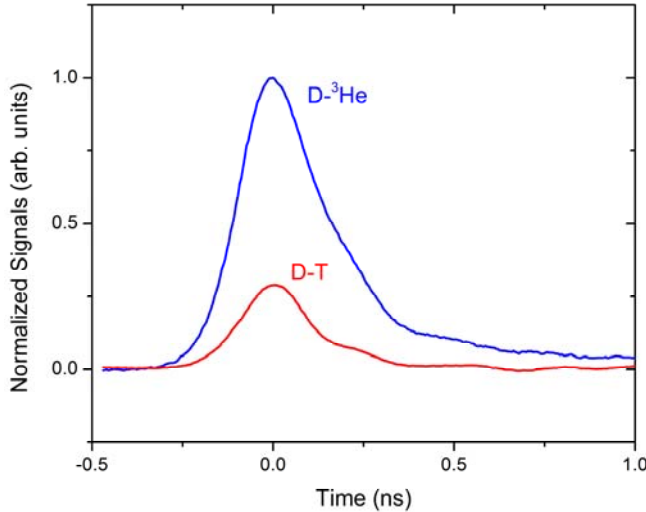


Figure 3: (Color online) (Top) A time trace of D-<sup>3</sup>He gamma-ray signal normalized by proton yield. (Bottom) A time trace of D-T gamma-ray signal normalized by neutron yield. These data indicate that the D-T  $\gamma/n$  branching ratio is  $\sim 1/3$  of the D-<sup>3</sup>He  $\gamma/p$  branching ratio.

The error weighted-average value for the D-T branching ratio over the two methods, absolute and cross-calibration, is  $(4.2 \pm 2.0) \times 10^{-5}$ . The current analysis incorporates the D-T fusion  $\gamma$ -ray emissions,  $\gamma_0$  and  $\gamma_1$ , and is shown in Figure 4 (red closed circle) as compared to earlier beam-target

results. On the right figure, Cecil *et al.* [5] data are plotted where only  $\gamma_0$  is considered and also Morgan *et al.* [6] data are plotted where Morgan *et al.* assumed that  $\gamma$ -ray data measured above 13.5 MeV did not contain any contribution from  $\gamma_1$ . In those measurements  $\gamma_1$  was obscured by the 14.1 MeV neutron-induced  $\gamma$ -ray background. Additionally, in thermal-equilibrium ICF plasmas, most of the nuclear reactions occur at the Gamow peak energy  $E_0$ , which for a D-T reaction can be written  $E_0 = 6.66(T_{ion})^{2/3}$  in the center of mass, where  $T_{ion}$  is the burn-averaged ion temperature in units of keV [29, 30]. For these D-T plastic capsule implosions at OMEGA,  $T_{ion}$  was 3 - 7 keV resulting in an  $E_0$  value of 14 - 24 keV. When translated to beam-target experimental conditions, these values correspond to an effective deuteron beam energy of  $E_d = 23 - 40$  keV, a value significantly lower than the deuteron beam energies previously reported from beam-target experiments.

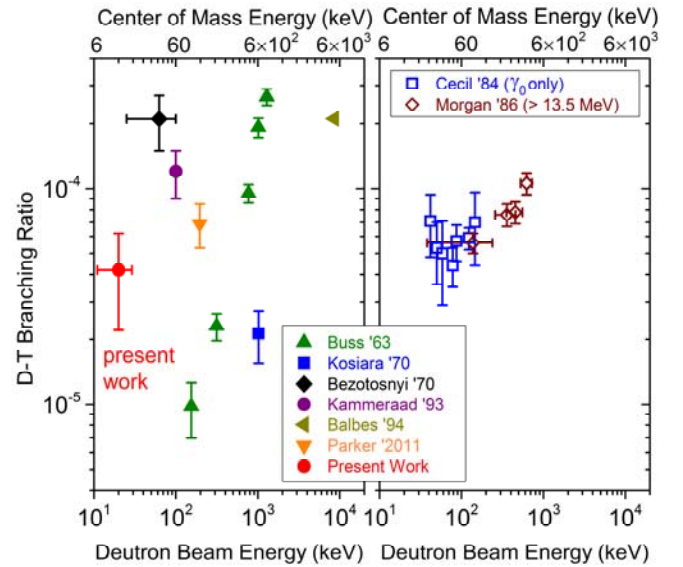


Figure 4: (Color) D-T branching ratio determined from this ICF implosion work (red closed circle) as compared to earlier work. Branching ratios shown in the left figure include  $\gamma_0$  and  $\gamma_1$  emissions, while only  $\gamma_0$  is considered in the right figure.

In order to interpret these experimental results, we assume the dominance of the  $3/2^+$  resonance in all reactions initiated by D+T at low energies. This leads to the theoretical expectation that the branching ratio is constant below about 100 keV center-of-mass energy, meaning that the ratio of Maxwellian averages of the cross sections at an ion temperature of 5 keV should not deviate significantly from the value seen at low energies in beam-target measurements. However, the expected energy dependence is evident only in the more recent beam-target measurements of Cecil *et al.* [5] and of Morgan *et al.* [6], which were measurements of the  $\gamma_0$  branch alone. Since their value for the  $\gamma_0$  transition barely overlaps the upper end of our error bar for the sum of  $\gamma_0 + \gamma_1$  transitions, the results cannot be considered consistent. This gives us cause for

further theoretical investigations of the D-T  $\gamma$ -ray spectrum, and of the energy dependence of the branching ratio, at low-energy ICF conditions. The  $\gamma$ -ray spectra were calculated using an approximation that neglects the recoil momentum of the photons, which should be corrected by using fully relativistic kinematics. The presence of other transitions in the  ${}^3\text{H}(\text{d}, \gamma)$  reaction at low energies in addition to the dominant  $3/2^+$  one could change the energy dependence of the branching ratio there. Such transitions have been observed in the polarization data of Riley *et al.* [31] and of Balbes *et al.* [11].

The observed difference in the  ${}^3\text{H}(\text{d}, \gamma){}^5\text{He}$  and  ${}^3\text{He}(\text{d}, \gamma){}^5\text{Li}$  branching ratios further motivates investigation of the multichannel  ${}^5\text{He}$ - and  ${}^5\text{Li}$ -system data simultaneously with a Coulomb-corrected, charge-symmetric R-matrix analysis. Such an analysis would impose the charge symmetry of the strong interactions by making the reduced-width amplitudes of the R-matrix levels the same in the two systems, while allowing the level energies in the two system to differ by an overall Coulomb shift. Additional Coulomb differences would come from the external relative wave functions (penetrability, *e.g.*) in the initial d+t and d+ ${}^3\text{He}$  channels, in the final n+ ${}^4\text{He}$  and p+ ${}^4\text{He}$  channels, and possibly in the photon widths of the  $\gamma$ + ${}^5\text{He}$  and  $\gamma$ + ${}^5\text{Li}$  channels due to the increased charge of  ${}^5\text{Li}$ . To attribute a ratio ( $B_{\gamma n}^{DT} / B_{\gamma p}^{D^3\text{He}}$ ) as low as approximately 0.3 purely to Coulomb effects would be a challenge for such an analysis, but is not beyond the realm of possibility. Therefore, we cannot at this point say whether the experimental result is evidence for charge-symmetry breaking without further theoretical analysis.

In summary, two methods have been employed to obtain the D-T gamma-to-neutron branching ratio by using ICF implosion experiments. Reduced background interferences over previous beam-target experiments and an improved understanding of the D-T  $\gamma$ -ray spectrum significantly lessen the uncertainties in the value. Averaging over the absolute and cross-calibration methods, a D-T branching ratio of  $(4.2 \pm 1.2) \times 10^{-5}$  has been determined at ICF conditions. Having D-T neutron and  $\gamma$ -ray measurements and the D- ${}^3\text{He}$  proton yields for this purpose allowed a unique determination of this fundamental nuclear property, and an improved understanding of theoretical predictions and previous measurements. This study illustrates the use of ICF implosions as a new platform in the emerging field of Plasma Nuclear Science [32] to augment traditional accelerator-based nuclear physics.

The authors thank the OMEGA and HiγS operations, engineering, and scientific staff who supported this work. This work was supported by LANL ICF Program, NLUF/DOE (Grant No. DE-FG03-03SF2269), and FSC/DOE (Grant No. DE-FC02-04ER54789).

[1] M. J. Edwards *et al.*, Phys. Plasmas **18**, 051003 (2011).  
[2] D. C. Wilson *et al.*, Rev. Sci. Instrum. **79**, 10E525 (2008).  
[3] F. Ajzenberg Selove, Nucl. Phys. A., **490**, 1 (1988).  
[4] J. M. Mack *et al.*, Radiat. Phys. Chem. **75**, 551 (2006).  
[5] F. E. Cecil *et al.*, Phys. Rev. Lett. **53** (8), 767 (1984).  
[6] G. L. Morgan *et al.*, Phys. Rev. C **33** (4), 1224 (1986).  
[7] J. E. Kammeraad *et al.*, Phys. Rev. C **47** (1), 29 (1993).

[8] W. Buss *et al.*, Phys. Lett. **4** (3), 198 (1963).  
[9] A. Kosiara *et al.*, Phys. Lett. **32B** (2), 99 (1970).  
[10] V. M. Bezotosny *et al.*, Sov. J. Nucl. Phys. **10** (3), 127 (1970).  
[11] M. J. Balbes *et al.*, Phys. Rev. C **49**, 912 (1994).  
[12] C. E. Parker, M.S. Thesis, Ohio University (2011).  
[13] J. Benveniste *et al.*, Nucl. Phys. **19**, 448 (1960).  
[14] G. Mitev *et al.*, Phys. Rev. C **34**, 389 (1986).  
[15] H. W. Herrmann *et al.*, Bulletin of the American Physical Society, 193 (2011).  
[16] R. A. August *et al.*, Phys. Rev. C **35**, 393 (1987).  
[17] R. R. Berggren *et al.*, Rev. Sci. Instrum. **72** (1), 873 (2001).  
[18] J. M. Mack *et al.*, Rev. Sci. Instrum. **77**, 10E728 (2006).  
[19] H. W. Herrmann *et al.*, Rev. Sci. Instrum. **79**, 10E531 (2008).  
[20] H. W. Herrmann *et al.*, J. Phys.: Conf. Ser. **244**, 032047 (2010).  
[21] H. W. Herrmann *et al.*, Rev. Sci. Instrum. **81**, 10D333 (2010).  
[22] V. Yu. Glebov *et al.*, Rev. Sci. Instrum. **75**, 3559 (2004).  
[23] A. Csoto *et al.*, Phys. Rev. C **55**, 536 (1997).  
[24] C. J. Horsfield *et al.*, Bulletin of the American Physical Society, 193 (2011).  
[25] M. S. Rubery *et al.*, Rev. Sci. Instrum. **81**, 10D328 (2010).  
[26] D. G. Hicks *et al.*, Phys. Plasmas **7** (12), 5106 (2000).  
[27] F. H. Seguin *et al.*, Rev. Sci. Instrum. **74** (2), 975 (2003).  
[28] F. E. Cecil *et al.*, Phys. Rev. C **32** (3), 690 (1985).  
[29] S. Atzeni *et al.*, The Physics of Inertial Fusion (2009).  
[30] D. T. Casey, Ph.D. Thesis, Massachusetts Institute of Technology (2012).  
[31] J. C. Riley *et al.*, Phys. Rev. C **40** (3), 1517 (1989).  
[32] J. A. Frenje *et al.*, Phys. Rev. Lett. **107**, 122502 (2011).